

Cite this paper: *Chin. J. Chem.* **2021**, *39*, 1517–1522. DOI: 10.1002/cjoc.202100013

Single-Component Chemical Nose with a Hemicyanine Probe for Pattern-Based Discrimination of Metal Ions[†]

 Jingying Zhai,^a Yaotian Wu,^b and Xiaojiang Xie^{*a,b}
^a Academy for Advanced Interdisciplinary Studies, Southern University of Science and Technology, Shenzhen, Guangdong 518055, China

^b Department of Chemistry, Southern University of Science and Technology, Shenzhen, Guangdong 518055, China

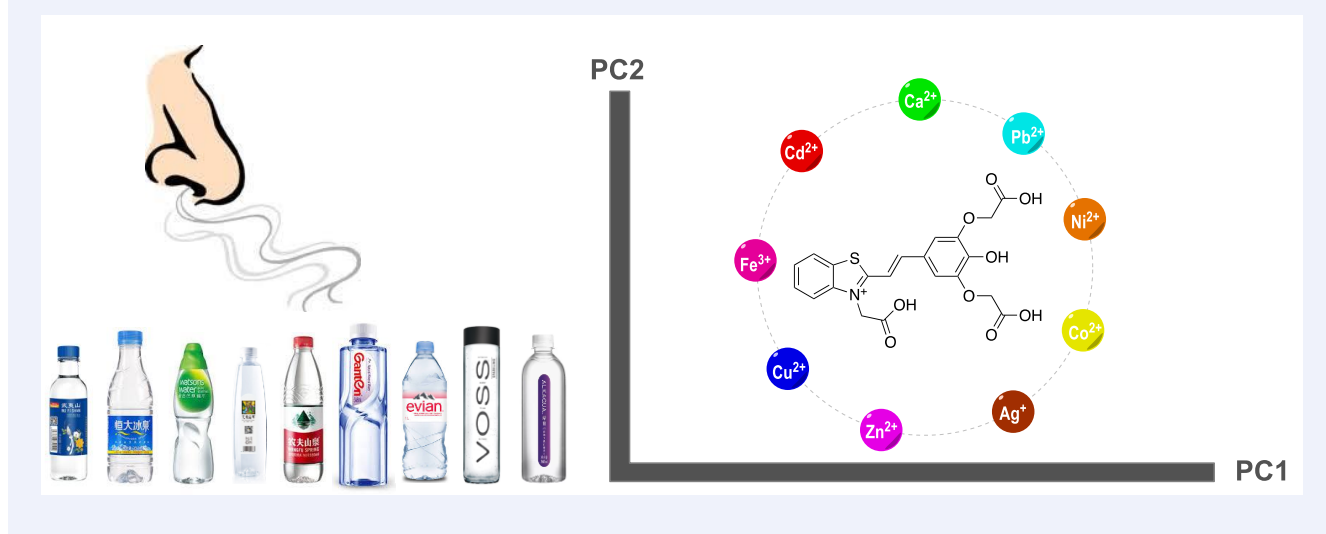
Keywords

Chemical nose | Cations | Sensors | UV/Vis spectroscopy | Principle component analysis

Main observation and conclusion

We report here a chemical nose utilizing the nonspecificity of a hemicyanine dye (probe P) containing three acetates and one deprotonatable phenol groups. Unlike conventional pattern-based recognition that requires a combination of different probes, probe P alone is able to differentiate 9 different metals, generating distinctive absorption spectra and various patterns upon principle component analysis (PCA). River water samples and commercial mineral water samples were evaluated by the probe and were successfully distinguished.

Comprehensive Graphic Content


^{*}E-mail: xiexj@sustech.edu.cn
[†] Dedicated to Department of Chemistry, SUSTech, on the Occasion of Her 10th Anniversary.

[View HTML Article](#)
[Supporting Information](#)

Background and Originality Content

Metal ions are ubiquitous in our daily life. They are crucial to human health and natural environment. Alkali metal ions such as Na^+ and K^+ maintain the water and electrolytes balance in our body.^[1-2] Alkaline earth metal ions such as Ca^{2+} and Mg^{2+} participate in skeletal development, nerve conduction, enzyme catalysis as well as gene transcription.^[3-6] Fe^{2+} , a central component of hemoglobin, takes part in the gas transport in blood.^[7] As for transitional metal ions (also referred to as heavy metal ions), a slight elevation in their concentration suffices to cause serious problems to the health of human beings as well as various ecological systems.^[8-9] Considering the important roles of metal ions, analytical tools are required so that ion concentrations could be readily measured. A number of analytical instruments serve for such a purpose, including ion chromatography, ion-selective electrodes, atomic spectroscopy, mass spectroscopy, electrophoresis, and so on.^[10-15] However, these instruments are cumbersome and require time-consuming sample preparation and pretreatment. To meet the escalating challenges in modern analytical chemistry, new methods suitable for real time and in-situ measurements are in urgent demand.

Synthetic probes are a family of chemosensors able to detect a range of analytes, including small molecules and ions.^[16-20] Colorimetry refers to the color changes that occur when the probe interacts with the analyte while fluorescence is the emission of light from the probe after it is brought to the excited state by light illumination. On the one hand, a number of synthetic probes have been reported with excellent selectivity to a certain target ion. A good selectivity allows the probe to detect the analyte in the presence of interfering species. On the other hand, the discovery of highly selective probes is usually a trial-and-error process, accompanied by countless unqualified products (typically regarded as failures) with non-specificity. Recently, scientists showed that such non-specific probes are after all not useless. On the contrary, when properly assembled, they could function resembling the olfactory systems of animals, leading to a unique analytical platform coined "chemical nose".^[21-23]

A chemical nose usually combines sensor arrays with statistical data analysis methods to qualitatively and quantitatively detect multiple analytes.^[24-28] Optical probes are widely used to form these sensor arrays and generate information-rich cross-responsive signals. By taking advantages of the well-established statistical methods such as principal component analysis (PCA) and hierarchical clustering analysis (HCA), the optical signals could be converted to more discriminate patterns.^[29] These characteristics make chemical nose capable of identification of various metal ions even with small change in complex samples. Chang and coworkers fabricate a sensors array composed of 5 fluorescent probes that can distinguish 7 heavy metal ions.^[30] Wolfbeis and coworkers made use of 8 different unselective indicators to form a sensor array to discriminate 5 metal ions.^[31] Chemical noses offer a good opportunity to discriminate different metal ions. However, the more the sensor elements, the more complex for the data acquisition and analysis. Some researchers make an effort to design sensor arrays with high separation ability but having minimal number of sensor elements. Recently, Pavel Anzenbacher and co-workers successfully reported a sensor assay with only one sensing element, a probe 8-hydroxyquinoline attached with conjugated fluorophore, which could discriminate 10 metal ions.^[32] Ding and coworkers reported a chemical nose using a surfactant assembled bis(2-picoyl)amine-modified pyrene derivative as the only sensing element, which could well differentiate 13 metal ions and different brands of drinking water.^[33] Du and coworkers reported a 1-(2-pyridinylazo)-2-naphthaleno (PAN)- and bromothymol blue (BTB)-functionalized microgel sensor array for colorimetric detection of 10 metal ions.^[34] However, in these reports dis-

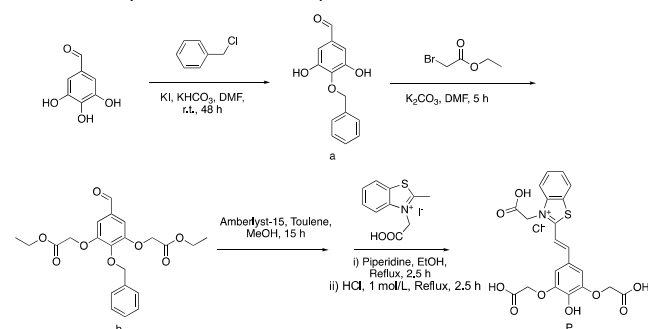
crimination of ions is achieved through embedding the probe in a complex environment. The probe itself is no doubt the key to maximize the capacity for discrimination. Here, we present a colorimetric chemical nose sensor with only one optical sensing element probe P. The probe contains a hemicyanine chromophore and multiple acetates and hydroxyl binding moieties, which generate information-rich absorption spectra during exposing to metal ions. The hydrophilic binding moieties also make this probe water soluble without needing embed into membrane, hydrogel or surfactants. By analysis of the absorbance data with principle component analysis (PCA) method, the probe is able to distinguish 9 metal ions, including Ca^{2+} , Co^{2+} , Cu^{2+} , Fe^{3+} , Zn^{2+} , Ag^+ , Ni^{2+} , Cd^{2+} , and Pb^{2+} . For practical applications, river samples were analyzed and 15 different brands of drinking water were satisfactorily differentiated with probe P.

Results and Discussion

Scheme 1 shows the synthetic route of the water soluble colorimetric probe P and the structure was confirmed with ^1H NMR and ^{13}C NMR (Figures S1 to S4). Probe P was designed with three acetates and one hydroxyl binding arms, which combine with a hemicyanine chromophore. The multiple binding arms are not specific for metal ions (similar with EDTA) and offer more possibility to generate numerous changes in optical signals when it binds with different metal ions. Also, the hydrophilic binding arms make this probe water soluble. These properties make probe P a good candidate as a chemical nose with simple sensing element. Binding with different cations will cause the deprotonation of the phenol group with different intramolecular charge transfer effect and thus generate optical spectroscopic changes.

The absorption spectra of probe P with different metal ions are shown in Figure 1a, including Ca^{2+} , Ag^+ , Cu^{2+} , Co^{2+} , Ni^{2+} , Cd^{2+} , Zn^{2+} , Pb^{2+} and Fe^{3+} . The experiments were performed at fixed pH (6.5) to avoid the pH interference. The absorption spectra of probe P are all red shift with diverse change in curve shape and absorbance (Figure 1a). At the same time, the color changes of probe P can be visualized by the naked eye from yellow (protonated form) to reddish (deprotonated form). Compared with different metal ions, the probe P shows distinct response with each other which are not specific to just one metal ion but multiple metal ions. This property makes probe P a promising chemical nose to identify various metal ions at the same time. For better visualization, the results were analyzed through principal component analysis (PCA). PCA is a statistical method able to reduce the data dimensions and find the most distinguishable components for differentiation. Usually, the largest degree principle component (PC1) of data variance and the second largest principle component (PC2) were used to plot the pattern 2-dimensionally. As shown in Figure 1b, the PC1 and PC2 were obtained based on Figure 1a and all of the 9 metal ions are satisfactorily distinguished.

Scheme 1 Synthetic route for the probe P in this work



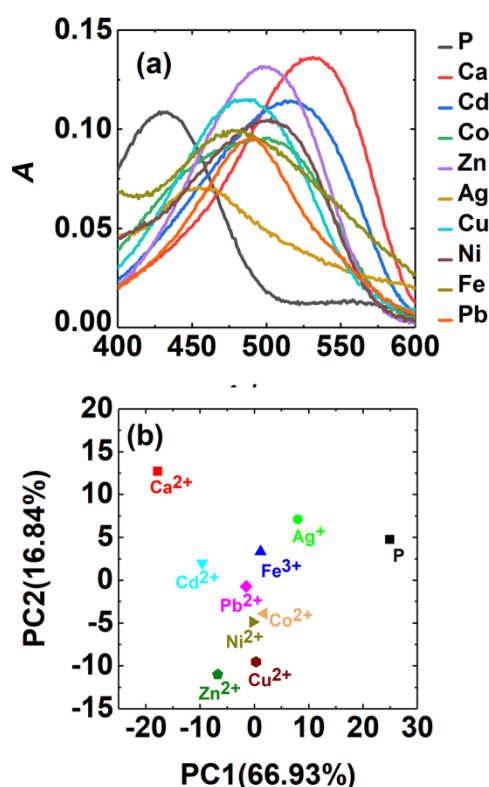


Figure 1 (a) UV-Vis spectra of probe P with 200 $\mu\text{mol/L}$ of metal ions in 5 mmol/L pH 6.5 MES-NaOH buffer solutions. (b) The corresponding PCA plot of Figure 1a. The concentration of P is kept at 3.33 $\mu\text{mol/L}$.

For metal ion detection, the affinity between the probe and the target ions is very important. The complex formation constants (K_f) for probe P and different metal ions were determined and summarized in Table 1. The constants were obtained through the calibration curves of probe P with different metal ions (Figure S5). The absorbance signals were recorded in MES-NaOH buffer solutions (pH 6.5, 5 mmol/L) and fixed P concentration (3.33×10^{-6} mol/L). The absorbance signals at 520 nm gradually increase with continuous adding of metal ions. Theoretical curves were used to fit the data to obtain the constants K_f (shown in Figure S5). The

Table 1 The complex formation constants K_f for probe P with different metal ions

Metal ion	$\lg K_f$
Pb^{2+}	6.15
Ca^{2+}	3.59
Cd^{2+}	4.25
Co^{2+}	3.43
Zn^{2+}	4.50
Ag^+	2.82
Cu^{2+}	5.23
Ni^{2+}	4.24
Fe^{3+}	4.40

results of K_f showed that probe P has satisfactory binding affinity and distinguishability to different metal ions. The affinity exhibited an order of $\text{Pb}^{2+} > \text{Cu}^{2+} > \text{Zn}^{2+} > \text{Fe}^{3+} > \text{Cd}^{2+} > \text{Ni}^{2+} > \text{Ca}^{2+} > \text{Co}^{2+} > \text{Ag}^+$. Other common cations such as Na^+ , K^+ , and Mg^{2+} were also tested up to 10 mmol/L, but they did not result in any spectral change.

The stoichiometry between probe P and the metal ion was obtained by the Job's method. In this method, the total concentration of probe and metal ion is fixed, but the mole fractions are varied. The maximum position (intercept of the two linear fittings) corresponds to the stoichiometry of the two species. Figure S6 demonstrates the Job's plot for probe P and different metal ions by plotting the absorbance with respect to the mole fraction of the two components. Except for Fe^{3+} and Ag^+ , the maxima position of Pb^{2+} , Cu^{2+} , Cd^{2+} , Ni^{2+} , Co^{2+} , Zn^{2+} , and Ca^{2+} are around at 0.5, which indicates the 1 to 1 stoichiometry for probe P and metal ions. The Job's plot curves are abnormal for Fe^{3+} and Ag^+ without showing maximum points. This might be due to the existence of ferric hydroxide at pH 6.5 and the detection limit of silver ions is quite high and beyond the normal association constant range.

To further quantitatively evaluate the response of probe P to metal ions, six metal ions were selected for the titration experiments. This is because probe P is relatively not very sensitive to Ag^+ and Ni^{2+} , and the concentration of Cd^{2+} in the real sample to be analyzed is expected very low. The absorption spectra were recorded with different ion concentrations during the performance of titration experiments as shown in Figure 2. Notably, the initial spectra without addition of metal ions are all the same, with

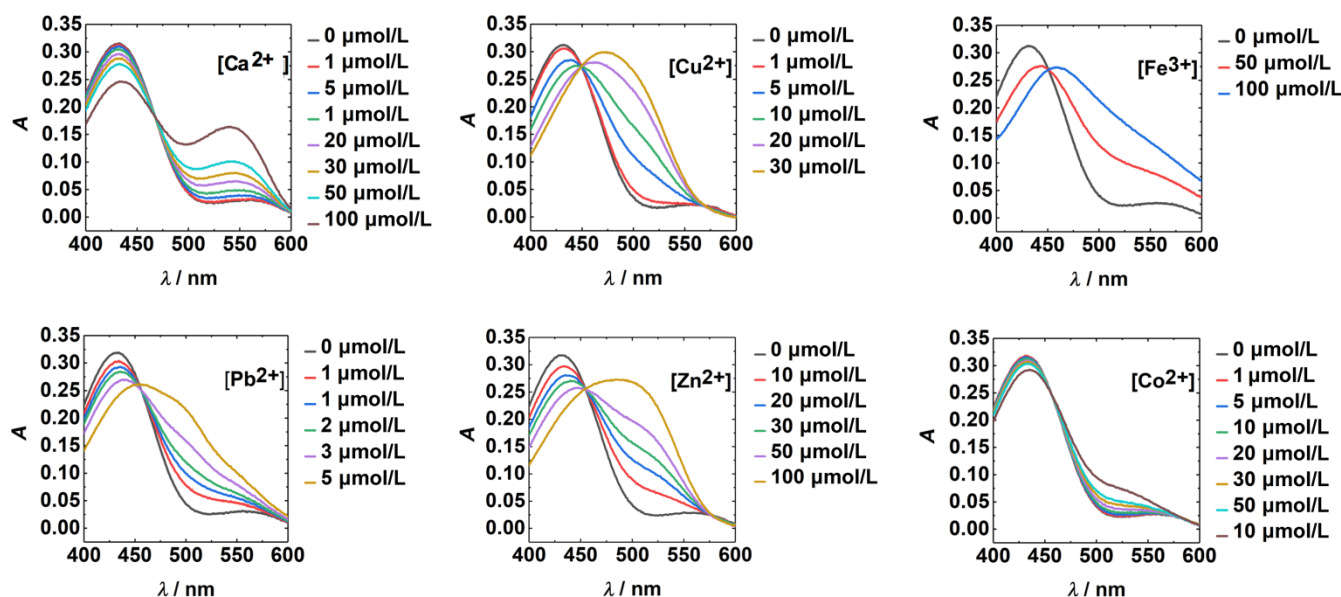


Figure 2 Absorbance response of probe P to Ca^{2+} , Cu^{2+} , Fe^{3+} , Pb^{2+} , Zn^{2+} and Co^{2+} with indicated concentrations in 5 mmol/L pH 6.5 MES-NaOH buffer solution. The concentration of P is kept at 3.33 $\mu\text{mol/L}$.

strong absorbance around 420 nm. With increasing metal ions, the spectra changed to different shapes by gradually decreasing at 420 nm and increasing at longer wavelength. The probe exhibited submicromolar detection limits depend on the nature of the ions.

The response of probe P to various concentrations of metal ions was also visualized with PCA in Figure 3a. The response started all from the same point representing P in the blank and dispersed to various directions. From the enlarged graph (Figure 3b), we could also visualize the separation of six metal ions at micromolar concentrations.

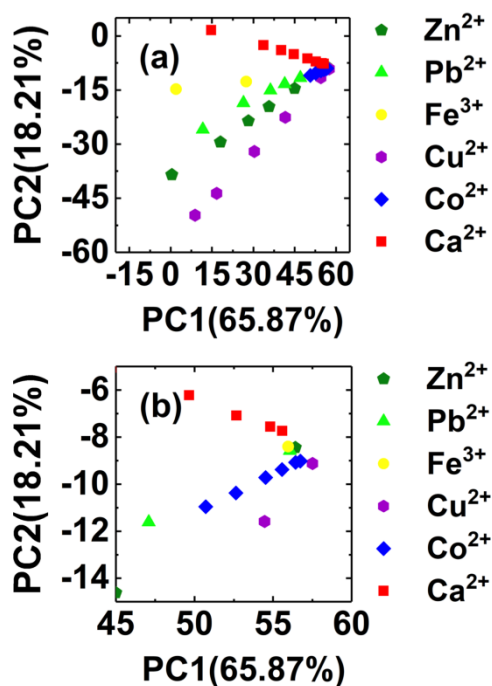


Figure 3 (a) The calibration curves of probe P with various metal ions in 5 mmol/L pH=6.5 MES-NaOH buffer solutions by using PCA method to analyze the absorption spectra. (b) The corresponding enlarged graph. The concentrations of different metal ions are as follows: Ca²⁺: 1, 5, 10, 20, 30, 50, 100 μmol/L; Co²⁺: 1, 5, 10, 20, 30, 50, 100 μmol/L; Cu²⁺: 1, 5, 10, 20, 30 μmol/L; Fe³⁺: 1, 50, 100 μmol/L; Zn²⁺: 10, 20, 30, 50, 100 μmol/L; Pb²⁺: 1, 1.5, 2, 3, 5 μmol/L.

To evaluate the ability of probe P to detect metal ions in real samples, five river samples from Dasha River, Shenzhen were gathered during different days and mixed with probe P in 5 mmol/L MES-NaOH pH=6.5 buffer solution. The absorbance signals were recorded and processed with the same principal components (PCs) vectors as calibration curves shown in Figure 4. All river water samples were located on the direction of Ca²⁺, implicating a high level of Ca²⁺ in the river water samples. Notice that the river water samples were collected at different time, which explains why the points are slightly dispersed in Figure 4. We then analyzed the samples by ion chromatography (IC) and atomic absorption spectroscopy (AAS). According to the IC data shown in Table 2, the major cations in river sample are Na⁺, Mg²⁺ and Ca²⁺. Other transition metal ions were found below the detection limit of IC, while the AAS showed extremely low concentration of Pb²⁺ below the detection limit of AAS (*ca.* 1 mg/L). Therefore, the contribution from the transition metal ions in the river water is considered negligible. Since probe P is not sensitive to Na⁺ and the level of heavy metal ions is low in the river samples, PCA of the sample should indeed locate on the calcium line.

Moreover, probe P was utilized to differentiate various brands of commercial drinking water. We purchased 14 different brands

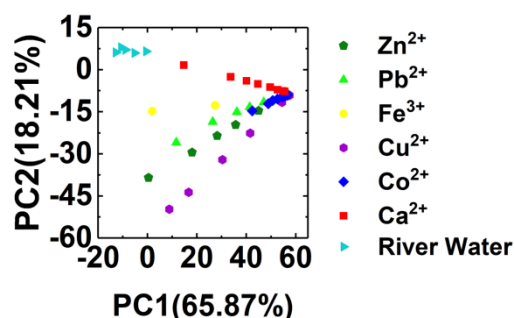


Figure 4 PCA diagram analysis of the river samples through calibration curves. Five river samples obtained from the same place at Dasha River, Shenzhen during different days. All the metal ions and samples were prepared with 5 mmol/L pH 6.5 MES-NaOH buffer solutions. Ca²⁺: 1, 5, 10, 20, 30, 50, 100 μmol/L; Co²⁺: 1, 5, 10, 20, 30, 50, 100 μmol/L; Cu²⁺: 1, 5, 10, 20, 30 μmol/L; Fe³⁺: 1, 50, 100 μmol/L; Zn²⁺: 10, 20, 30, 50, 100 μmol/L; Pb²⁺: 1, 1.5, 2, 3, 5 μmol/L.

Table 2 Ion chromatograph results of the river sample

Metal ions	Concentration/(mg·L ⁻¹)
Na ⁺	1.556
Mg ²⁺	0.228
Ca ²⁺	3.247

of mineral water including 1 tap water sample obtained directly from the lab. PCA analyses of the water samples are shown in Figure 5. The experiments were easily performed by dissolving P in different water samples without dilution or pretreatment. The spectra were analyzed with the abovementioned PCA method and the results showed that all the 15 kinds of drink water could be well separated. Distinguishing the samples was successful mainly due to the various concentrations of Ca²⁺ and pH, providing a two co-ordination for each sample. Since Ca²⁺ and pH are very important parameters for commercial mineral water, we believe that this simple chemical nose could potentially serve as an easy-to-use quality control reagent.

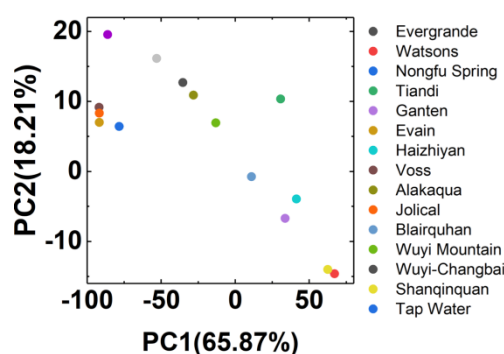


Figure 5 The PCA diagram of probe P in response to 15 brands of drinking water.

Conclusions

In this article, we reported a colorimetric probe P with the ability to generate information-rich spectra upon binding with various metal ions. The nonspecific binding enabled the probe as a chemical nose to differentiate 9 metal ions including Ca²⁺, Ag⁺, Cu²⁺, Co²⁺, Ni²⁺, Cd²⁺, Zn²⁺, Pb²⁺ and Fe³⁺. PCA was engaged to provide clear visualization of the detection. Analyzing real water samples with the probe led to the finding of high level of Ca²⁺

which agreed well with IC and AAS. 14 different commercial mineral water and tap water were also successfully distinguished.

Experimental

Reagents. Cd(NO₃)₂·4H₂O, Ni(NO₃)₂·6H₂O, CuCl₂, ZnCl₂, FeCl₃·6H₂O, MgCl₂·6H₂O, CoCl₂·6H₂O, Pb(NO₃)₂, CaCl₂·6H₂O, AgNO₃, NaCl, KHCO₃, KI, 2-(*N*-morpholino)ethanesulfonic acid (MES), 3-ethyl-2-methylbenzothiazolium iodide, benzyl chloride, 3,4,5-trihydroxybenzaldehyde, ethyl bromoacetate, amberlyst-15 and all the metal ion salts used were purchased from Sigma-Aldrich. Piperidine was purchased from Shanghai Lingfeng Chemical Reagent Co., Ltd. Ethanol was purchased from Shanghai Titan Scientific Co., Ltd.

Instrumentation and measurements. Ultraviolet–visible (UV–vis) absorption spectra were measured using an absorption spectrometer (Evolution 220, Thermo Fisher Scientific). Ion chromatography was measured on the model Eco IC with Metrosep C 6 – 150/4.0 from Metrohm. Atomic spectra were measured by atomic absorption spectrometer (AA400, Perkin Elmer). All solutions except those specifically mentioned were prepared by dissolving appropriate salts into deionized water purified by Milli-Q Integral 5.

Identification of stoichiometry between probe P and metal ions by Job's Plot approach. 100 μmol/L P and 100 μmol/L metal ions were prepared for Job's Plot experiment by using 5 mmol/L MES–NaOH buffer solution (pH = 6.5). The Job's Plot experiment was performed by mixing P and metal ions. The mole fractions of P were varied from 0 to 1 with fixed total concentrations of P and metal ion. The corresponding UV–Vis absorption spectra were recorded and the absorbance at 520 nm was used for analysis of the metal-to-P stoichiometry.

Measurement of complex formation constants between probe P and metal ions. The complex formation constants were obtained through the calibration curves of metal ions with probe P in absorbance mode. The experiments were performed under fixed P concentration (3.33 × 10⁻⁶ mol/L) with different metal ion concentration at pH 6.5 (5 mmol/L MES–NaOH buffer solution).

Identification of different brands of drinking water. 9 mL of different brand drinking water was mixed with 1 mL of 10⁻⁴ mol/L P, respectively. Then the absorbance was recorded and analyzed by PCA through the software Wolfram Mathematica.

Measurement of UV-Vis spectrum of P with river water sample. The river water sample obtained from Dasha River, Shenzhen was filtered by the 0.22 μm syringe filter to remove the particulates. After adjusting the pH to 6.5 with MES–NaOH, the stock solution of P at 3.33 × 10⁻⁴ mol/L was diluted 100 times with the abovementioned river water samples. Finally, the absorbance signals were measured by UV–Vis spectroscopy.

Supporting Information

The supporting information for this article is available on the WWW under <https://doi.org/10.1002/cjoc.202100013>.

Acknowledgement

We thank the technical support from SUSTech Core Research Facilities. This work is financially supported and dedicated to the 10th anniversary of SUSTech.

References

- [1] Reinert, M.; Khaldi, A.; Zauner, A.; Doppenberg, E.; Choi, S.; Bullock, R. High Level of Extracellular Potassium and Its Correlates after Severe Human Head Injury: Relationship to High Intracranial Pressure. *J. Neurosurg.* **2000**, *93*, 800–807.
- [2] Terry, J. The Major Electrolytes: Sodium, Potassium, and Chloride. *J. Intraven. Nurs.* **1994**, *17*, 240–247.
- [3] Clapham, D. E. Calcium Signaling. *Cell* **2007**, *131*, 1047–1058.
- [4] Kuchibhotla, K. V.; Lattarulo, C. R.; Hyman, B. T.; Bacskai, B. J. Synchronous Hyperactivity and Intercellular Calcium Waves in Astrocytes in Alzheimer Mice. *Science* **2009**, *323*, 1211–1215.
- [5] Lee, T.-S.; Radak, B. K.; Harris, M. E.; York, D. M. A Two-Metal-Ion-Mediated Conformational Switching Pathway for HDV Ribozyme Activation. *ACS Catal.* **2016**, *6*, 1853–1869.
- [6] Bischof, H.; Burgstaller, S.; Waldeck-Weiermair, M.; Rauter, T.; Schinagl, M.; Ramadani-Muja, J.; Graier, W. F.; Malli, R. Live-Cell Imaging of Physiologically Relevant Metal Ions Using Genetically Encoded FRET-Based Probes. *Cells* **2019**, *8*, 492–516.
- [7] Jensen, K. P.; Ryde, U. How O₂ Binds to Heme: Reasons for Rapid Binding and Spin Inversion. *J. Biol. Chem.* **2004**, *279*, 14561–14569.
- [8] Kumar, P. N.; Dushenkov, V.; Motto, H.; Raskin, I. Phytoextraction: The Use of Plants to Remove Heavy Metals from Soils. *Environ. Sci. Technol.* **1995**, *29*, 1232–1238.
- [9] Jiang, Y.; Liu, C.; Huang, A. EDTA-Functionalized Covalent Organic Framework for the Removal of Heavy-Metal Ions. *ACS Appl. Mater. Interfaces* **2019**, *11*, 32186–32191.
- [10] Zhou, Q.; Lei, M.; Liu, Y.; Wu, Y.; Yuan, Y. Simultaneous Determination of Cadmium, Lead and Mercury Ions at Trace Level by Magnetic Solid Phase Extraction with Fe@Ag@Dimercaptobenzene Coupled to High Performance Liquid Chromatography. *Talanta* **2017**, *175*, 194–199.
- [11] Vortmann-Westhoven, B.; Diehl, M.; Winter, M.; Nowak, S. Ion Chromatography with Post-column Reaction and Serial Conductivity and Spectrophotometric Detection Method Development for Quantification of Transition Metal Dissolution in Lithium Ion Battery Electrolytes. *Chromatographia* **2018**, *81*, 995–1002.
- [12] Neu, H. M.; Lee, M.; Pritts, J. D.; Sherman, A. R.; Michel, S. L. J. Seeing the "Unseeable", A Student-Led Activity to Identify Metals in Drinking Water. *J. Chem. Educ.* **2020**, *97*, 3690–3696.
- [13] Zhao, L.; Jiang, Y.; Wei, H.; Jiang, Y.; Ma, W.; Zheng, W.; Cao, A.-M.; Mao, L. In Vivo Measurement of Calcium Ion with Solid-State Ion-Selective Electrode by Using Shelled Hollow Carbon Nanospheres as a Transducing Layer. *Anal. Chem.* **2019**, *91*, 4421–4428.
- [14] Liu, C.; Bi, X.; Zhang, A.; Qi, B.; Yan, S. Preparation of an L-Cysteine Functionalized Magnetic Nanosorbent for the Sensitive Quantification of Heavy Metal Ions in Food by Graphite Furnace Atomic Absorption Spectrometry. *Anal. Lett.* **2020**, *53*, 2079–2095.
- [15] Song, X.; Zhang, R.; Wang, Y.; Feng, M.; Zhang, H.; Wang, S.; Cao, J.; Xie, T. Simultaneous Determination of Five Metal Ions by On-Line Complexion Combined with Micelle to Solvent Stacking in Capillary Electrophoresis. *Talanta* **2020**, *209*, 120578–120585.
- [16] Paolesse, R.; Nardis, S.; Monti, D.; Stefanelli, M.; Natale, C. D. Porphyrinoids for Chemical Sensor Applications. *Chem. Rev.* **2017**, *117*, 2517–2583.
- [17] Chen, X.; Nam, S.-W.; Jou, M. J.; Kim, Y.; Kim, S.-J.; Park, S.; Yoon, J. Hg²⁺ Selective Fluorescent and Colorimetric Sensor: Its Crystal Structure and Application to Bioimaging. *Org. Lett.* **2008**, *10*, 5235–5238.
- [18] Zhang, H.; Han, L.-F.; Zachariasse, K. A.; Jiang, Y.-B. 8-Hydroxyquinoline Benzoates as Highly Sensitive Fluorescent Chemosensors for Transition Metal Ions. *Org. Lett.* **2005**, *7*, 4217–4220.
- [19] Gong, Y.-J.; Zhang, X.-B.; Zhang, C.-C.; Luo, A.-L.; Fu, T.; Tan, W.; Shen, G.-L.; Yu, R.-Q. Through Bond Energy Transfer: A Convenient and Universal Strategy toward Efficient Ratiometric Fluorescent Probe for Bioimaging Applications. *Anal. Chem.* **2012**, *84*, 10777–10784.
- [20] Zhu, C.; Huang, M.; Lan, J.; Chung, L. W.; Li, X.; Xie, X. Colorimetric Calcium Probe with Comparison to an Ion-Selective Optode. *ACS Omega* **2018**, *3*, 12476–12481.
- [21] Geng, Y.; Peveler, W. J.; Rotello, V. M. Array-based "Chemical Nose"

- Sensing in Diagnostics and Drug Discovery. *Angew. Chem. Int. Ed.* **2019**, *58*, 5190–5200.
- [22] Li, Z.; Askim, J. R.; Suslick, K. S. The Optoelectronic Nose: Colorimetric and Fluorometric Sensor Arrays. *Chem. Rev.* **2019**, *119*, 231–292.
- [23] Mallet, A. M.; Davis, A. B.; Davis, D. R.; Panella, J.; Wallace, K. J.; Bonizzoni, M. A Cross Reactive Sensor Array to Probe Divalent Metal Ions. *Chem. Commun.* **2015**, *51*, 16948–16951.
- [24] Liu, Y.; Mettry, M.; Gill, A. D.; Perez, L.; Zhong, W.; Hooley, R. J. Selective Heavy Element Sensing with a Simple Host-Guest Fluorescent Array. *Anal. Chem.* **2017**, *89*, 11113–11121.
- [25] Li, X.; Li, S.; Liu, Q.; Chen, Z. Electronic-Tongue Colorimetric-Sensor Array for Discrimination and Quantitation of Metal Ions Based on Gold-Nanoparticle Aggregation. *Anal. Chem.* **2019**, *91*, 6315–6320.
- [26] Lee, J. W.; Lee, J.-S.; Kang, M.; Su, A. I.; Chang, Y.-T. Visual Artificial Tongue for Quantitative Metal-Cation Analysis by an Off-the-Shelf Dye Array. *Chem. – Eur. J.* **2006**, *12*, 5691–5696.
- [27] Wang, Z.; Palacios, M. A.; Pavel Anzenbacher, J. Fluorescence Sensor Array for Metal Ion Detection Based on Various Coordination Chemistries: General Performance and Potential Application. *Anal. Chem.* **2008**, *80*, 7451–7459.
- [28] Xue, S.-F.; Chen, Z.-H.; Han, X.-Y.; Lin, Z.-Y.; Wang, Q.-X.; Zhang, M.; Shi, G. DNA Encountering Terbium(III): A Smart “Chemical Nose/Tongue” for Large-Scale Time-Gated Luminescent and Lifetime-Based Sensing. *Anal. Chem.* **2018**, *90*, 3443–3451.
- [29] Jolliffe, I. T. *Principal Component Analysis*, Springer, New York, **1986**.
- [30] Xu, W.; Ren, C.; Teoh, C. L.; Peng, J.; Gadre, S. H.; Rhee, H.-W.; Lee, C.-L. K.; Chang, Y.-T. An Artificial Tongue Fluorescent Sensor Array for Identification and Quantitation of Various Heavy Metal Ions. *Anal. Chem.* **2014**, *86*, 8763–8769.
- [31] Mayr, T.; Igel, C.; Liebsch, G.; Klimant, I.; Wolfbeis, O. S. Cross-Reactive Metal Ion Sensor Array in a Micro Titer Plate Format. *Anal. Chem.* **2003**, *75*, 4389–4396.
- [32] Palacios, M. A.; Wang, Z.; Montes, V. A.; Zyryanov, G. V.; Pavel Anzenbacher, J. Rational Design of a Minimal Size Sensor Array for Metal Ion Detection. *J. Am. Chem. Soc.* **2008**, *130*, 10307–10314.
- [33] Zhang, L.; Huang, X.; Cao, Y.; Xin, Y.; Ding, L. Fluorescent Binary Ensemble Based on Pyrene Derivative and Sodium Dodecyl Sulfate Assemblies as a Chemical Tongue for Discriminating Metal Ions and Brand Water. *ACS Sens.* **2017**, *2*, 1821–1830.
- [34] Zhou, X.; Nie, J.; Du, B. Functionalized Ionic Microgel Sensor Array for Colorimetric Detection and Discrimination of Metal Ions. *ACS Appl. Mater. Interfaces* **2017**, *9*, 20913–20921.

Manuscript received: January 4, 2021

Manuscript revised: February 4, 2021

Manuscript accepted: February 5, 2021

Accepted manuscript online: February 7, 2021

Version of record online: XXXX, 2021